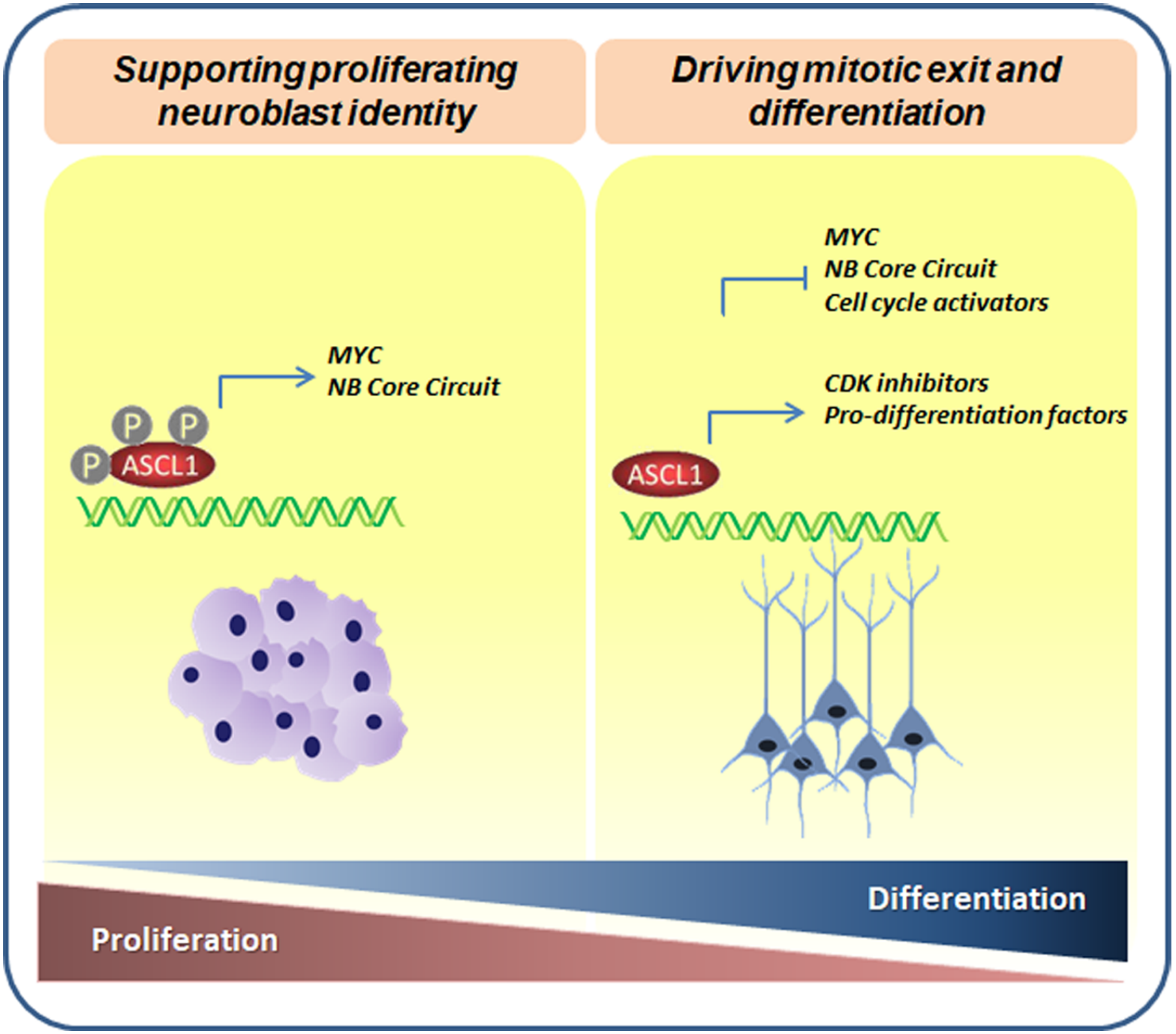
Supporting proliferating neuroblast identity
Driving mitotic exit and differentiation
MYC
NB Core Circuit
P
P
P
ASCL1
MYC
NB Core Circuit
Cell cycle activators
CDK inhibitors
Pro-differentiation factors
ASCL1
Differentiation
Proliferation

Dephosphorylation of the proneural transcription factor ASCL1 re-engages a latent post-mitotic differentiation programme in neuroblastoma

Fahad R. Ali[1,2,3,¶], Daniel Marcos[1,2,¶], Igor Chernukhin[4], Laura M. Woods[1,2], Lydia M. Parkinson [1,2], Luke A. Wylie[1], Tatiana D. Papkovskaia[1], John D. Davies[1,2], Jason S. Carroll[4], Anna Philpott [1,2*]

[1]Department of Oncology, University of Cambridge, Cambridge, UK

[2]Wellcome-MRC Cambridge Stem Cell Institute, Jeffrey Cheah Biomedical Centre, Cambridge Biomedical Campus, Puddicombe Way, Cambridge, UK

[3]College of Medicine, Mohammed Bin Rashid University of Medicine and Health Sciences, Dubai, United Arab Emirates

[4]Cancer Research UK Cambridge Institute, University of Cambridge, Robinson Way, Cambridge, UK

[¶] These authors contributed equally

*Correspondence: ap113@cam.ac.uk

Running Title: ASCL1 dephosphorylation drives neuroblastoma differentiation

Financial Support

Work was supported by Cancer Research UK Programme Grant RG91505 (AP), Wellcome Trust Investigator Award 212253/Z/18/Z (AP), MRC Research Grant MR/L021129/1 (F.A, A.P); Neuroblastoma UK (D.M, T.P, A.P), CRUK Cambridge Centre Paediatric Programme (L.P), The Terry Fox Foundation (FA), MBRU College of Medicine Internal grant award MBRU-CM-RG2019-14 (FA), MBRU-ALMAHMEED Collaborative Research Award ALM1909 (FA) and core support from the Wellcome Trust and the MRC Cambridge Stem Cell Institute (F.A, D.M, J.D., A.P.) and Cancer Research UK Cambridge Insititute (I.C, J.C).

Conflict of interest

The authors declare no competing interests.

Abstract

Paediatric cancers often resemble trapped developmental intermediate states that fail to engage the normal differentiation programme, typified by high-risk neuroblastoma arising from the developing sympathetic nervous system. Neuroblastoma cells resemble arrested neuroblasts trapped by a stable but aberant epigenetic programme controlled by sustained expression of a core transcriptional circuit of developmental regulators in conjunction with elevated MYCN or MYC (*MYC*). The transcription factor ASCL1 is a key master regulator in neuroblastoma and has oncogenic and tumour suppressive activities in several other tumour types. Using functional mutational approaches, we find that preventing CDK-dependent phosphorylation of ASCL1 in neuroblastoma cells drives co-ordinated suppression of the MYC-driven core circuit supporting neuroblast identity and proliferation, while simultaneously activating an enduring gene programme driving mitotic exit and neuronal differentiation.

Implications: These findings indicate that targeting phosphorylation of ASCL1 may offer a new approach to development of differentiation therapies in neuroblastoma.

Introduction

Neuroblastoma tumour cells resemble malignant neuroblastic developmental intermediates trapped epigenetically in a precursor-like state (1). In common with other childhood tumours that arise from aberrant proliferation of developmental intermediates, reactivation of a latent developmental programme of mitotic exit and differentiation may provide a promising therapeutic approach (2); for instance, reactivation of differentiation in the paediatric malignancy acute promyelocytic leukaemia has transformed the outcome of this disease from a frequently fatal disease to one with a 90% cure rate (3). Directed reactivation of tumour cell differentiation requires an understanding of the molecular mechanisms that cause stalling of normal development and an ability to reverse that stalling.

In neuroblastoma, recent studies have supported a model of aberrant epigenetic control that locks cells in a progenitor-like state via a network of super-enhancers; genes associated with an early developmental and proliferative programme are highly expressed because of associated and mutually regulated oncogenic super-enhancers (4-8). High level of expression of these genes is maintained by elevated super-enhancer-associated MYCN or c-MYC particularly in disease with poor prognosis. While collapse of this super-enhancer network by targeting transcriptional CDKs can lead to neuroblastoma cell death (9), reactivating the normal developmental processes in neuroblastoma cells is likely to require a more directed approach and modulation of the activity of transcriptional regulators that usually control these processes during development. One such regulator is ASCL1, a bHLH proneural transcription factor that plays a central role in noradrenergic neuron differentiation.

ASCL1 regulates both neural stem cell maintenance and differentiation during embryonic development (10), while its expression can be associated with cancer "stem-ness" in glioblastoma (11, 12), small cell lung carcinoma (13), medulloblastoma (14) and

neuroblastoma (15-17). Conversely in glioblastoma, enhancing ASCL1 activity by Notch inhibition is sufficient to promote cell cycle exit and attenuate tumourigenicity (12). Therefore, evidence from the developing and adult central nervous system as well as glioblastoma indicates that ASCL1 levels, and therefore activity, may be critical for determining whether ASCL1 supports stem/progenitor maintenance or drives differentiation (10, 12).

Building on our understanding of the regulation of ASCL1 protein in normal development (15, 18), here we show that preventing ASCL1 phosphorylation in neuroblastoma cells results in cell cycle exit by direct suppression of the neuroblastic core regulatory circuit and the target genes that drive cell cycle progression. Alongside a supression of this pro-proliferative programme, we find that un(der)phosphorylated ASCL1 simultaneously activates expression of the CDK inhibitor CDKN1C as well as genes associated with neuronal differentiation and function, driving mitotic exit and morphological maturation. Thus, we show that post-translational activation of a key developmental regulator in cancer cells can unmask latent tumour suppressive activity, inhibiting proliferation and promoting differentiation.

Materials and Methods

Cell lines

The Neuroblastoma cell line SH-SY5Y was kindly gifted by Prof. John Hardy, UCL, and the SK-N-BE(2)c cell line was kindly gifted by Prof. Deborah Tweddle, Newcastle University. Cells were verified by submitting genomic DNA for short tandem repeat (STR) sequencing and compared to the Children's Oncology Group Cell Line Identification database (http://www.cogcell.org/clid.php) to ensure it was genetically matched to standardised cell lines. All cell lines were confirmed to be free of mycoplasma prior to use and were tested

every three months. All cell lines were cultured in DMEM/F-12 with GlutaMAX™ supplement, 10% tetracycline-free Fetal Bovine Serum (Clontech), and 100 units/ml penicillin and 100 µg/ml streptomycin. Lenti-X™ 293T cell line was cultured in DMEM/F-12 with GlutaMAX™ supplement, 10% tetracycline-free Fetal Bovine Serum (Clontech), and 100 units/ml penicillin and 100 µg/ml streptomycin.

Generation of Lentivirally Transduced Cell Lines

Lentivirally-transduced lines were generated using the pLVX-CMV-Tet3G system, detailed method is available as an associated file at the GEO database https://www.ncbi.nlm.nih.gov/geo/ and assigned the identifier GSE153823.

Proliferation Assays

Proliferation assays were performed in the Incucyte analysis system (IncuCyte Zoom™ Videomicroscopy, Essen Bioscience Ltd.). Relative confluency was calculated by comparing growth rates of either WT or SA ASCL1 versus uninduced cells. Cell count experiments were carried out in parallel to evaluate total cell numbers at different time points. Briefly, cell numbers of two independent clones of each of WT and S-A SH-SY5Y were compared to uninduced clonal cell lines. (SH-SY5Y cells were induced with 4ng/mL doxycycline over 96 hours).

Chromatin isolation, Western Blotting and Phos-Tag Western Blot

Subcellular fractionation was performed using the subcellular protein fractionation kit (Thermo Scientific) according to the manufacturer's instructions. Western blot analysis were performed as previously described in (19). ASCL1 phospho-status was determined in 8% acrylamide gels polymerised with 20 µM Phos-tag reagent (WAKO) and 40 µM MnCl2.

After running and before transfer, phos-tag gels were washed three times, 10 min each with transfer buffer (25mM Tris-HCl, 190mM glycine, 20% methanol) plus 10 mM EDTA, followed by a final wash with transfer buffer. Antibodies used were: anti-ASCL1 (1:250; a kind gift from David Anderson and Francois Guillemot), anti-C-MYC (1:10000; Abcam), anti- N-MYC (1:500; Abcam), anti-H3 (1:5000; Abcam), anti-PARP (1:500; BD) and anti-GAPDH (1:1000; Sigma) or anti α-tubulin (1:5000; Sigma).

Immunohistochemistry

Immunohistochemistry was performed as previously described in (19). Antibodies used were anti-β tubulin (TUJ1) (1:1000; Covance) or anti-ASCL1 (1:200; Abcam).

Quantitative Real-Time PCR

Quantitative real-time PCR was perfomed as previously described in (19). The primer sequences are provided in Supplementary Table 1. Relative quantification was determined according to the ΔΔc(t) method. Data are presented as means ± S.E.M. of normalised values.

Chromatin Immunoprecipitation (ChIP), ChIP-Seq

ChIP and ChIPseq were performed as described previously (20, 21). Antibodies used were anti-ASCL1 (Abcam) and anti-IgG (Abcam). ChiPSeq data and full associated methods are both available as an associated file at the GEO database https://www.ncbi.nlm.nih.gov/geo/ and assigned the identifier GSE153823. ChIPseq experiments were performed in two separate clones of each of WT and S-A SH-SY5Y tetracycline-inducible stable cell lines induced with 1 μg/ml doxycycline for 24 hours in four biological replicates. Differential binding analysis (Diffbind) was performed as described previously (20). ChIP-qPCR primer sequences are provided in Supplementary Table S1.

RNA-seq

RNA-sequencing experiments were performed in SH-SY5Y, WT and S-A SH-SY5Y tetracycline-inducible stable cell lines, using two clones of each in at least five biological replicates for each cell line. Full RNAseq data and methods for RNA-seq are available at the GEO database https://www.ncbi.nlm.nih.gov/geo/ and assigned the identifier GSE153823. Single-end 50-bp reads generated on the Illumina HiSeq sequencer were aligned to the human genome version GRCh37 and read counts were generated using STAR 2.5.1a (22).

Gene Set Enrichment Analysis

FDR-values derived from DESeq2 analyses of the RNA-Seq data for all selected genes were –log10 transformed. These values were subsequently used for ranking and weighting of genes. GSEA Preranked analysis tool from Gene Set Enrichment Analysis (GSEA) software, version 2.2.3 (http://software.broadinstitute.org/gsea/index.jsp) has been used for establishing potential functional relation in gene expression.

Quantification and statistical analysis

Statistical analysis were performed using a two-tailed unpaired student t-test (*P≤0.05, **P≤0.01, ***P≤0.001); standard error of the mean (S.E.M.) calculated from at least three independent experiments.

Data availability

The next generation sequencing data from this publication have been deposited to the GEO database https://www.ncbi.nlm.nih.gov/geo/ and assigned the identifier GSE153823.

Results

Elevated ASCL1 activity promotes mitotic exit of neuroblastoma cells

Neuroblastoma cells frequently express ASCL1 (15), yet remain highly proliferative. As over-expression of ASCL1 can drive ectopic noradrenergic neurogenesis *in vivo* (15), we questioned whether an increase in ASCL1 activity over the endogenous level might be sufficient to render neuroblastoma cells post-mitotic and activate morphological differentiation. To explore this, we exploited the SH-SY5Y neuroblastoma cell line, which expresses a moderate level of ASCL1 protein (15) and is a representative model of the higher risk ADRN disease subtype (4, 5) (hereafter NB cells). Using isogenically matched ASCL1-inducible NB lines to study the effects of different expression levels (Supplementary Fig. S1A) revealed that increasing WT ASCL1 progressively reduced NB cell confluency (Supplementary Fig. S1B). Cell apoptosis is accompanied by cleavage of PARP, which can be readily observed after SDS PAGE separation in control NB cells treated with the apoptotic inducer Staurosporine (Supplementary Fig. S1C). A PARP cleavage product is absent from Dox-treated ASCL1-expressing NB cells, so the reduction in cell number cannot be attributed to an increase in apoptosis, but does indicate that elevating ASCL1 activity supresses NB cell proliferation.

A phosphomutant form of ASCL1 (S-A ASCL1) can be generated by mutating all serine-proline phosphorylation sites to alanine-proline. This phosphomutant form of the protein has previously been used to show that preventing multi-site phosphorylation of ASCL1 promotes transcription factor-mediated reprogramming of embryonic ectoderm and fibroblasts into neurons (18). When expressed in NB cells and detected by western blotting after SDS PAGE separation, S-A ASCL1 runs faster than WT ASCL1 but with similar mobility to WT ASCL1 that has been exposed to a broad-spectrum phosphatase,

(Supplementary Fig. S1D). This indicates that extensive ASCL1 phosphorylation in NB cells usually occurs on serine-proline sites and is prevented by introducing phosphorylation site mutations. We next tested whether preventing phosphorylation of ASCL1 on serine-proline sites in NB cells affects its ability to potentiate cell cycle exit and differentiation.

Un(der)phosphorylated ASCL1 drives cell cycle exit and differentiation

To directly compare the effect of increasing ectopic expression of either wild-type or phospho-mutant ASCL1 in NB cells, we induced ASCL1 protein in doxycycline-inducible clonal cell lines expressing either WT or S-A ASCL1 (Fig. 1A and Supplementary Figure S1B), resulting in nuclear expression of ASCL1 (Supplementary Fig. S1E). When induced at similar levels in NB cells, phosphomutant S-A ASCL1 shows greater potency in suppressing cell division than WT ASCL1 (Figure 1A left, Supplementary Fig. S1B). Proliferative arrest induced by S-A ASCL1 is accompanied by cell aggregation, and also neurite extension normally associated with neuronal differentiation (Fig. 1A, right). Over-expression of S-A ASCL1 also drives neurite extension in BE(2)C cells, a MYCN-amplified neuroblastoma cell line, while expression of WT ASCL1 at a similar level does not (Supplementary Figure 1F).

To understand how un(der)phosphorylated ASCL1 inhibits neuroblastoma proliferation and enhances changes associated with differentiation, we interrogated RNAseq data to identify changes in expression of selected key regulators 24 hours post WT and SA-ASCL1-expression, alongside ChIPseq data quantifying ASCL1 binding adjacent to regulated genes. S-A ASCL1 binds more effectively that WT ASCL1 to regulatory regions associated with several prominent pro-proliferative genes including *SKP2*, *E2F1* and the *MYC*-target gene *CDCA7* and also downregulates their expression (Fig. 1B), as further validated by ChIP-qPCR and real-time PCR analysis (Fig. 1C and 1D). Other key cell cycle regulators

including CDK1 and CDK2 are also highly downregulated by un(der)phosphorylated ASCL1 (Fig. 1D).

Un(der)phosphorylated ASCL1 inhibits the MYC-driven core regulatory circuit that drives neuroblastoma.

ADRN-type neuroblastoma is locked into a highly proliferative state by a core oncogenic network of transcription factors, representing the "core regulatory circuit" (4, 5). This includes the developmental regulators *PHOX2B*, *HAND2* and *GATA3* that combinatorially activate high level expression of each other and of downstream target genes via clusters of regulatory elements called "super-enhancers" (4, 5). Importantly, ASCL1 binds in proximity to the genomic locations that encode all three of these genes, suggesting feed-forward regulatory mechanisms (17). We investigated the effect of elevated WT or S-A ASCL1 on expression of these core regulatory circuit (CRC) genes. Upregulation of WT ASCL1 results in a modest suppression of the CRC genes GATA3 and HAND2, while having little effect on PHOX2B, whereas S-A ASCL1 induction results in almost total suppression of expression of all 3 of these CRC genes (Fig. 2A).

c-MYC/NMYC binds at super-enhancers associated with the *PHOX2B*/*HAND2*/*GATA3* core regulatory circuit and are associated with particularly high levels of gene activation (4). High risk neuroblastoma can have either MYCN amplification (23), or alternatively elevated MYC (*MYC*). Elevated MYC functions in place of NMYC in our SH-SY5Y NB cell model to maintain their neuroblastic phenotype (24). Consistent with a role for NMYC amplification being replaced by MYC activity in SH-SY5Y cells, we see that NMYC is cytoplasmic (Supplementary Fig. S2A). Moreover, MYCN is known to be directly regulated by ASCL1 in MYCN-amplified cell lines (17), while *MYCN* gene expression is not altered by WT or S-A ASCL1 in NB cells (Supplementary Fig. S2B), which

is also consistent with MYC and not MYCN regulating the neuroblastic programme in SH-SY5Y NB cells. We therefore investigated the effect of ASCL1 on MYC expression and its chromatin association in NB cells.

Both WT and S-A ASCL1 bind the *MYC* gene locus and S-A ASCL1 in particular suppresses MYC expression (Fig. 2A). S-A ASCL1 induction also results in reduced C-MYC binding to NB cell chromatin (Fig. 2B and Supplementary Fig. S2C), and consistent with this, S-A ASCL1 induction significantly perturbs the expression of hallmark MYC target genes (Fig. 2C), as well as downregulating genes associated with cell cycle phase transitions (Fig. 2C).

In addition to suppressing pro-proliferative genes, and the core regulatory circuit that maintains the proliferating neuroblastic phenotype, ASCL1 also binds and activates expression of the CDK inhibitor CDKN1C (Fig. 3A). Thus S-A ASCL1 can directly drive cell cycle exit by co-ordinated downregulation of the MYC-driven core regulatory circuit that maintains neuroblast identity as well as regulating genes that control the cell cycle directly. This is in contrast to WT ASCL1 which shows less repressive activity on MYC and other key cell cycle target genes.

Decreased proliferation of NB cells could be a consequence of a switch to a pro-differentiation state. In support of this hypothesis, we saw that increased ASCL1 activity, and particularly that of phospho-mutant S-A ASCL1, results in enhanced binding and activation of a wide range of direct targets that have previously been associated with neuronal differentiation (Fig. 3A and Supplementary Fig. S3) (25-27), with further expression validation undertaken by ChIP-qPCR and real-time PCR analysis (Fig. 3B and 3C).

We next explored whether the programme of ASCL1-induced mitotic arrest is reversible in SH-SY5Y NB cells. When S-A ASCL1 was induced at low levels, marked

suppression of cell division was observed (Fig. 1A, Supplementary Figure 1B and Figure 3D). When we removed doxycycline after 4 days to turn off expression of S-A ASCL1, we saw a rapid re-entry into cell cycle (Fig. 3D). However, when S-A ASCL1 was expressed continuously for 7 days and then turned off, the re-entry into the cell cycle was substantially slower (Fig. 3D), demonstrating that post-mitotic effects of prolonged expression of un(der)phosphorylated ASCL1 are relatively durable even after ASCL1 removal.

Discussion

ADRN-type neuroblastoma, the most lethal form of the disease, is driven by high level expression of the core regulatory circuit of transcription factors including *PHOX2B*, *HAND2* and *GATA3* (4, 5). These factors are usually transiently expressed in sympathetic neuron development, but elevated MYCN and/or MYC results in stabilisation of mutually regulated super-enhancers associated with these and other genes that lock cells in a pro-proliferative neuroblastic phenotype (6, 24). Indeed, deregulated MYCN has been directly shown to invade enhancers of developmentally-regulated genes, locking cells in pre-established progenitor behaviour epigenetically (7). Here we show that activation of ASCL1 by dephosphorylation drives a direct programme of mitotic arrest and gene expression changes consistent with differentiation in neuroblastoma cells that carry high levels of MYC, as well as promoting cell aggregation and neurite outgrowth (Figure 1A). High risk disease is often associated with MYCN gene amplification and the BE(2)C cell line, representative of this class of neuroblastomas, also shows signs of neurite extension in response to phosphomutant ASCL1 (Supplementary Figure 1F). Neuroblastoma is a highly diverse disease. It will be important to to further explore ASCL1's potential as a therapeutic target in this devastating disease by determining which subtypes of neuroblastoma respond to dephosphorylated ASCL1 by undergoing mitotic exit and differentiation.

ASCL1 is expressed in ADRN-type neuroblastoma (5, 17), where selective pressures may favour a level lower of ASCL1 than the threshold required to drive cell cycle exit and differentiation (Supplementary Figure S1B). We show enhancing ASCL1 activity by dephosphorylation can unlock a latent ability of NB cells to exit the cell cycle and undergo differentiation manifested in transcriptional and morphological changes, in part by co-ordinately downregulating the MYC-driven *PHOX2B*/*GATA3*/*HAND2* core regulatory circuit that drives the pro-proliferative oncogenic ADRN phenotype of NB cells. In addition, un(der)phosphorylated ASCL1 simultaneously directly suppresses pro-proliferative targets such as *SKP2* and *E2F1* and activates the CDK inhibitor CDKN1C, resulting in exit from cell cycle, as well as activating a programme of genes associated with neuronal development and differentiation.

Elevating ASCL1 expression level in the subset of glioblastoma stem cells that usually express ASCL1 only at a low level is sufficient to drive stable cell cycle exit (12). High levels of ASCL1 also impair reversion to a self renewing state even when ASCL1 is subsequently turned off (12), mimicking its normal role in development and pointing to a wider ability of ASCL1 to drive a stable state of differentiation in malignant cells. Our data in neuroblastoma cells indicate that activation of ASCL1 may also be achieved by preventing its phosphorylation. ASCL1 has been shown to be phosphorylated by cyclin-dependent kinases in developing Xenopus embryos (18) and by MAP kinases in glioma cells (28). Rapidly proliferating neuroblastoma cells are likely to have high level of both classes of kinases, so CDK inhibitors and MAP kinase inhibitors are good candidates, perhaps in combination, to drive differentiation of neuroblastomas by dephosphorylation of endogenous ASCL1, and it will be important to now test this *in vivo*. We also note that investigation of trials of CDK4/6-targeted CDKis as therapeutic agents in neuroblastoma are already underway (29) and possible effects on differentiation as well as mitotic exit/cell death should

be explored. There is also interest in the therapeutic use of CDK inhibitors that primarily target the transcriptional CDKs , CDK7/9 (9). These appear to bring about cell death by targeting the high level expression of the CRC genes and MYCN mediated by high level super-enhancer activity. We note that inhibitors that generally repress transcription are very likely to impede re-imposition of a differentiation programme, so inhibitors with specificity for mitotic CDKs are better candidates for use in therapies designed to promote differentiation.

Proneural transcription factors are increasingly identified as playing a crucial role in lineage-specific oncogenesis. For example, ASCL1 is expressed in a number of tumours including neuroblastoma, glioblastoma and small cell lung cancer (11, 13, 15, 16), while other proneural proteins act in an oncogenic context in medulloblastoma, and many endocrine neoplasias (2, 30). The relative importance of these proneural factors in defining the cell of origin and context of oncogenic drivers versus an active role in driving tumorigenicity is generally unclear (2), although an active pro-tumorigenic function is likely in some contexts; for instance, ASCL1 transcriptionally upregulates oncogenic and anti-apoptotic drivers such as MYCL1, SOX2, NF-IB, and BCL2 in small cell lung cancer (13, 31).

While, a picture is emerging in multiple cancers of the function of these master regulator proneural factors being subverted to promote oncogenesis, their activity in tumours still retains echoes of their normal developmental role in controlling the balance between proliferation and differentiation (2, 30). Phosphorylation of proneural proteins is a widely-conserved regulatory mechanism controlling the differentiation activity of many members of this transcription factor family in development (e.g. (18, 19, 32, 33)). In neuroblastoma cells, we see that a more normal developmental function of driving differentiation can be re-imposed on ASCL1 protein by manipulating its post-translational modification. We propose a wider model that the phosphorylation of proneural factors by elevated CDKs and other

proline-directed kinases in rapidly dividing cancer cells may act in multiple tumour types to profoundly affect the spectrum of proneural target gene expression, favouring those that potentiate stem/progenitor maintenance, rather than those that would drive differentiation. Given ASCL1's role supporting oncogenesis in other cancers (11, 13, 15, 16, 34), and the fact that different types of aggressive tumours converge on a neuroendocrine identity that is associated with enhanced accessibility of ASCL1-responsive elements (35), it is tempting to speculate that inhibiting ASCL1 phosphorylation could be exploited to drive differentiation for therapeutic benefit in a range of cancers.

Acknowledgements

We would like to sincerely thank Sabine Dietmann, Mohammadmersad Ghorbani for help with bio-informatic analysis, Geetha Sankaranarayanan for technical support. Carol Thiele, Louis Chesler, John Gurdon, Guy Blanchard, Clive DeSantos, Eva Papachristou and all Philpott lab members for helpful discussions. We would like to thank Prof. Deborah Tweddle and Prof. John Hardy for generously supplying the neuroblastoma cell lines. Work was supported by Cancer Research UK Programme Grant RG91505 (AP), Wellcome Trust Investigator Award 212253/Z/18/Z (AP), MRC Research Grant MR/L021129/1 (F.A, A.P); Neuroblastoma UK (D.M, T.P, A.P), CRUK Cambridge Centre Paediatric Programme (L.P), The Terry Fox Foundation (FA), MBRU College of Medicine Internal grant award MBRU-CM-RG2019-14 (FA), MBRU-ALMAHMEED Collaborative Research Award ALM1909 (FA) and core support from the Wellcome Trust and the MRC Cambridge Stem Cell Institute (F.A, D.M, J.D., A.P.) and Cancer Research UK Cambridge Insititute (I.C, J.C).

Author contributions

F.A., D.M, L.W and L.P developed experimental protocols, performed and analysed experiments with assistance from J.D. I.C. performed bioinformatic analysis. T.P., D.M., and L.W. generated the cell lines. All authors contributed to discussions. A.P. and J.C. directed the project, designed experiments, interpreted results and A.P. wrote the manuscript.

References

1. Ratner N, Brodeur GM, Dale RC, Schor NF. The "neuro" of neuroblastoma: Neuroblastoma as a neurodevelopmental disorder. Ann Neurol. 2016;80(1):13-23.
2. Azzarelli R, Simons BD, Philpott A. The developmental origin of brain tumours: a cellular and molecular framework. Development. 2018;145(10).
3. de The H, Chen Z. Acute promyelocytic leukaemia: novel insights into the mechanisms of cure. Nat Rev Cancer. 2010;10(11):775-83.
4. Boeva V, Louis-Brennetot C, Peltier A, Durand S, Pierre-Eugene C, Raynal V, et al. Heterogeneity of neuroblastoma cell identity defined by transcriptional circuitries. Nat Genet. 2017;49(9):1408-13.
5. van Groningen T, Koster J, Valentijn LJ, Zwijnenburg DA, Akogul N, Hasselt NE, et al. Neuroblastoma is composed of two super-enhancer-associated differentiation states. Nat Genet. 2017;49(8):1261-6.
6. Durbin AD, Zimmerman MW, Dharia NV, Abraham BJ, Iniguez AB, Weichert-Leahey N, et al. Selective gene dependencies in MYCN-amplified neuroblastoma include the core transcriptional regulatory circuitry. Nat Genet. 2018;50(9):1240-6.
7. Zeid R, Lawlor MA, Poon E, Reyes JM, Fulciniti M, Lopez MA, et al. Enhancer invasion shapes MYCN-dependent transcriptional amplification in neuroblastoma. Nat Genet. 2018;50(4):515-23.
8. van Groningen T, Akogul N, Westerhout EM, Chan A, Hasselt NE, Zwijnenburg DA, et al. A NOTCH feed-forward loop drives reprogramming from adrenergic to mesenchymal state in neuroblastoma. Nat Commun. 2019;10(1):1530.
9. Chipumuro E, Marco E, Christensen CL, Kwiatkowski N, Zhang T, Hatheway CM, et al. CDK7 inhibition suppresses super-enhancer-linked oncogenic transcription in MYCN-driven cancer. Cell. 2014;159(5):1126-39.
10. Castro DS, Martynoga B, Parras C, Ramesh V, Pacary E, Johnston C, et al. A novel function of the proneural factor Ascl1 in progenitor proliferation identified by genome-wide characterization of its targets. Genes Dev. 2011;25(9):930-45.
11. Rheinbay E, Suva ML, Gillespie SM, Wakimoto H, Patel AP, Shahid M, et al. An aberrant transcription factor network essential for Wnt signaling and stem cell maintenance in glioblastoma. Cell Rep. 2013;3(5):1567-79.
12. Park NI, Guilhamon P, Desai K, McAdam RF, Langille E, O'Connor M, et al. ASCL1 Reorganizes Chromatin to Direct Neuronal Fate and Suppress Tumorigenicity of Glioblastoma Stem Cells. Cell Stem Cell. 2017;21(2):209-24 e7.
13. Sabari JK, Lok BH, Laird JH, Poirier JT, Rudin CM. Unravelling the biology of SCLC: implications for therapy. Nat Rev Clin Oncol. 2017;14(9):549-61.
14. Ayrault O, Zhao H, Zindy F, Qu C, Sherr CJ, Roussel MF. Atoh1 inhibits neuronal differentiation and collaborates with Gli1 to generate medulloblastoma-initiating cells. Cancer Res. 2010;70(13):5618-27.
15. Wylie LA, Hardwick LJ, Papkovskaia TD, Thiele CJ, Philpott A. Ascl1 phospho-status regulates neuronal differentiation in a Xenopus developmental model of neuroblastoma. Dis Model Mech. 2015;8(5):429-41.
16. Kasim M, Hess V, Scholz H, Persson PB, Fahling M. Achaete-Scute Homolog 1 Expression Controls Cellular Differentiation of Neuroblastoma. Front Mol Neurosci. 2016;9:156.

17. Wang L, Tan TK, Durbin AD, Zimmerman MW, Abraham BJ, Tan SH, et al. ASCL1 is a MYCN- and LMO1-dependent member of the adrenergic neuroblastoma core regulatory circuitry. Nat Commun. 2019;10(1):5622.
18. Ali FR, Cheng K, Kirwan P, Metcalfe S, Livesey FJ, Barker RA, et al. The phosphorylation status of Ascl1 is a key determinant of neuronal differentiation and maturation in vivo and in vitro. Development. 2014;141(11):2216-24.
19. Ali F, Hindley C, McDowell G, Deibler R, Jones A, Kirschner M, et al. Cell cycle-regulated multi-site phosphorylation of Neurogenin 2 coordinates cell cycling with differentiation during neurogenesis. Development. 2011;138(19):4267-77.
20. Jozwik KM, Chernukhin I, Serandour AA, Nagarajan S, Carroll JS. FOXA1 Directs H3K4 Monomethylation at Enhancers via Recruitment of the Methyltransferase MLL3. Cell Rep. 2016;17(10):2715-23.
21. Schmidt D, Wilson MD, Spyrou C, Brown GD, Hadfield J, Odom DT. ChIP-seq: using high-throughput sequencing to discover protein-DNA interactions. Methods. 2009;48(3):240-8.
22. Anders S, Huber W. Differential expression analysis for sequence count data. Genome Biol. 2010;11(10):R106.
23. Huang M, Weiss WA. Neuroblastoma and MYCN. Cold Spring Harb Perspect Med. 2013;3(10):a014415.
24. Zimmerman MW, Liu Y, He S, Durbin AD, Abraham BJ, Easton J, et al. MYC Drives a Subset of High-Risk Pediatric Neuroblastomas and Is Activated through Mechanisms Including Enhancer Hijacking and Focal Enhancer Amplification. Cancer Discov. 2018;8(3):320-35.
25. Constantinescu R, Constantinescu AT, Reichmann H, Janetzky B. Neuronal differentiation and long-term culture of the human neuroblastoma line SH-SY5Y. J Neural Transm Suppl. 2007(72):17-28.
26. Kovalevich J, Langford D. Considerations for the use of SH-SY5Y neuroblastoma cells in neurobiology. Methods Mol Biol. 2013;1078:9-21.
27. Shipley MM, Mangold CA, Szpara ML. Differentiation of the SH-SY5Y Human Neuroblastoma Cell Line. J Vis Exp. 2016(108):53193.
28. Li S, Mattar P, Dixit R, Lawn SO, Wilkinson G, Kinch C, et al. RAS/ERK signaling controls proneural genetic programs in cortical development and gliomagenesis. J Neurosci. 2014;34(6):2169-90.
29. Geoerger B, Bourdeaut F, DuBois SG, Fischer M, Geller JI, Gottardo NG, et al. A Phase I Study of the CDK4/6 Inhibitor Ribociclib (LEE011) in Pediatric Patients with Malignant Rhabdoid Tumors, Neuroblastoma, and Other Solid Tumors. Clin Cancer Res. 2017;23(10):2433-41.
30. Huang C, Chan JA, Schuurmans C. Proneural bHLH genes in development and disease. Curr Top Dev Biol. 2014;110:75-127.
31. Augustyn A, Borromeo M, Wang T, Fujimoto J, Shao C, Dospoy PD, et al. ASCL1 is a lineage oncogene providing therapeutic targets for high-grade neuroendocrine lung cancers. Proc Natl Acad Sci U S A. 2014;111(41):14788-93.
32. Azzarelli R, Hurley C, Sznurkowska MK, Rulands S, Hardwick L, Gamper I, et al. Multi-site Neurogenin3 Phosphorylation Controls Pancreatic Endocrine Differentiation. Dev Cell. 2017;41(3):274-86 e5.

33. Tomic G, Morrissey E, Kozar S, Ben-Moshe S, Hoyle A, Azzarelli R, et al. Phospho-regulation of ATOH1 Is Required for Plasticity of Secretory Progenitors and Tissue Regeneration. Cell Stem Cell. 2018;23(3):436-43 e7.
34. Rapa I, Volante M, Migliore C, Farsetti A, Berruti A, Vittorio Scagliotti G, et al. Human ASH-1 promotes neuroendocrine differentiation in androgen deprivation conditions and interferes with androgen responsiveness in prostate cancer cells. Prostate. 2013;73(11):1241-9.
35. Park JW, Lee JK, Sheu KM, Wang L, Balanis NG, Nguyen K, et al. Reprogramming normal human epithelial tissues to a common, lethal neuroendocrine cancer lineage. Science. 2018;362(6410):91-5.

Figure Legends

Fig 1: ASCL1 expression and phosphorylation regulates NB cell proliferation

(A) Cell count assay of WT versus S-A ASCL1 NB cells after doxycycline induction at 4ng/ml, n=3 biological replicates. Graph shows Mean ± SEM, two-tailed unpaired t-test (***p<0.001) [Left]. Cell clustering and neurite outgrowth (white arrow heads) after WT and S-A ASCL1 induction. Tuj1 staining (Green), DAPI (Blue) [Right].

(B) ChipSeq and RNAseq tracks of pro-proliferative targets *SKP2*, *E2F1* and *CDCA7* in NB cells, either uninduced (Ctl) or 24 hours post-induction of WT and S-A ASCL1. ChipSeq n=8 in 4 biological replicates, RNAseq n=10 in 5 biological replicates.

(C) ChIP qPCR of *SKP2*, *E2F1* and *CDCA7* in NB cells 24 hours post-induction of WT and S-A ASCL1, n=4 biological replicates. Graph shows Mean ± SEM, two-tailed unpaired t-test (*** p<0.001).

(D) qPCR analysis of pro-proliferative targets in NB cells either uninduced (control) or 24 hours post-induction of WT and S-A ASCL1, n=4 biological replicates. Graph shows Mean ± SEM, two-tailed unpaired t-test (*** p<0.001).

Fig 2: Dephosphorylated ASCL1 supresses the oncogenic core regulatory circuit of NB cells

(A) ChIPseq and RNAseq tracks of *PHOX2B*, *GATA3*, *HAND2* and *MYC* in NB cells, either uninduced (Ctl) or 24 hours post-induction of WT and S-A ASCL1. ChipSeq n=8 in 4 biological replicates, RNAseq n=10 in 5 biological replicates.

(B) Western blotting for MYC within the cytoplasm and chromatin fractions either uninduced (Ctl) or 24 hours post-induction of WT and S-A ASCL1, GAPDH (control for cytoplasmic fractionation) and histone H3 (control for chromatin fractionation).

(C) Gene set enrichment analysis (GSEA Preranked) of downregulated gene sets after an evaluated differential gene expression test of S-A ASCL1 versus uninduced cells. The ranked gene list was tested against Hallmarks or Gene Ontology set from the GSEA database.

Fig 3: Dephosphorylated ASCL1 unlocks a latent ability of NB cells to differentiate

(A) ChipSeq and RNAseq tracks of differentiation targets in NB cells, either uninduced (Ctl) or 24 hours post-induction of WT and S-A ASCL1. ChipSeq n=8 in 4 biological replicates, RNAseq n=10 in 5 biological replicates.

(B) ChIP qPCR of differentiation targets in NB cells 24 hours post-induction of WT and S-A ASCL1, n=4 biological replicates. Graph shows Mean ± SEM, two-tailed unpaired t-test (*$p<0.05$, **$p<0.01$, *** $p<0.001$)

(C) qPCR analysis of differentiation targets in NB cells either uninduced (control) or 24 hours post-induction of WT and S-A ASCL1, n=4 biological replicates. Graph shows Mean ± SEM, two-tailed unpaired t-test (*** $p<0.001$).

(D) Cell count after S-A ASCL1 induction by addition of 4ng doxycycline for 96 hrs or 7 days as labelled, doxycycline removed for 1, 3 and 7 days, as labelled. n=6 in 3 biological replicates. Graph shows Mean ± SEM, two-tailed unpaired t-test. (**$p < 0.01$).

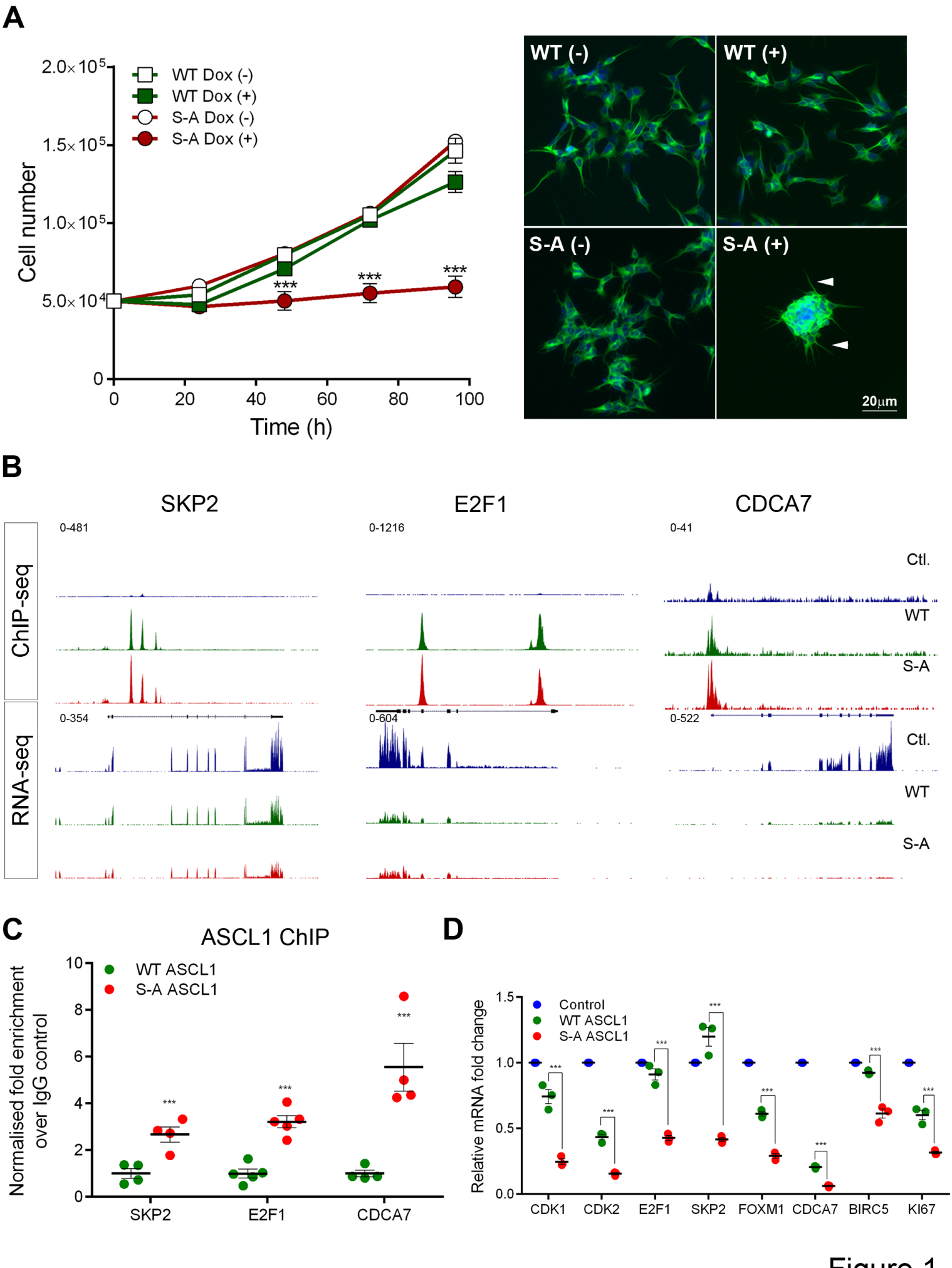
A
Cell number
Time (h)
WT Dox (-)
WT Dox (+)
S-A Dox (-)
S-A Dox (+)
***
WT (-)
WT (+)
S-A (-)
S-A (+)
20μm
B
SKP2
E2F1
CDCA7
ChIP-seq
RNA-seq
0-481
0-1216
0-41
0-354
0-604
0-522
Ctl.
WT
S-A
C
ASCL1 ChIP
Normalised fold enrichment over IgG control
WT ASCL1
S-A ASCL1
SKP2
E2F1
CDCA7
D
Relative mRNA fold change
Control
WT ASCL1
S-A ASCL1
CDK1
CDK2
E2F1
SKP2
FOXM1
CDCA7
BIRC5
KI67

Figure 1

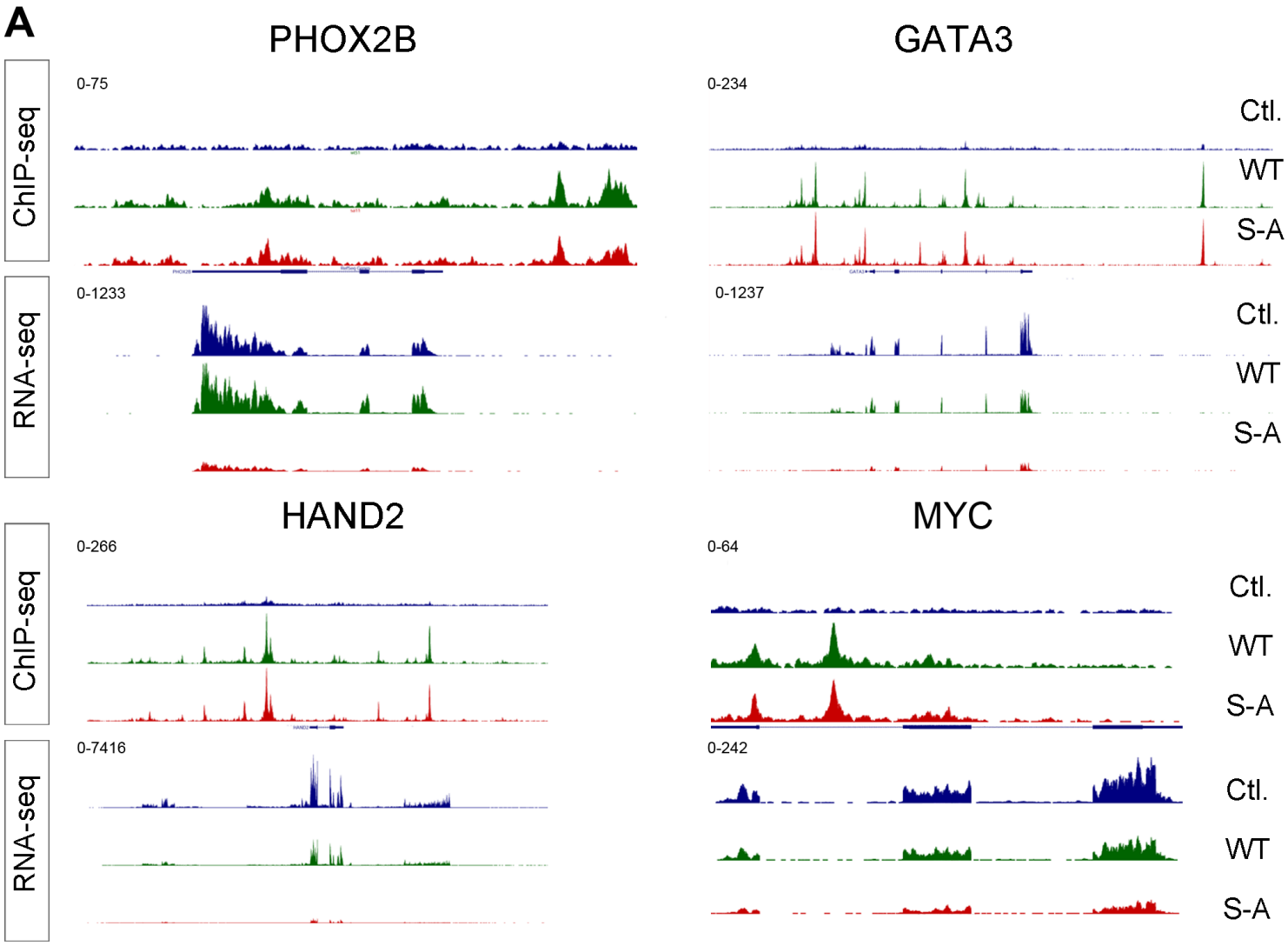
A
PHOX2B
GATA3
ChIP-seq
RNA-seq
0-75
0-234
0-1233
0-1237
Ctl.
WT
S-A
HAND2
MYC
0-266
0-64
0-7416
0-242

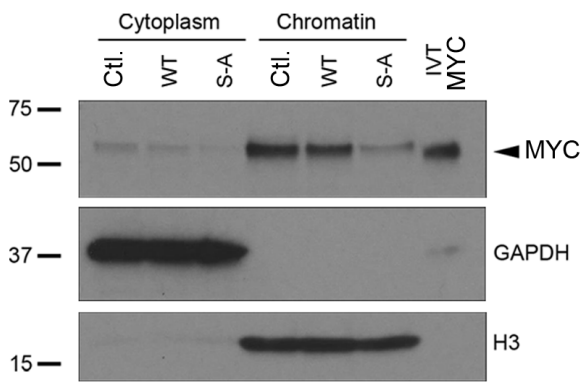
B
Cytoplasm
Chromatin
Ctl.
WT
S-A
IVT MYC
75
50
37
15
MYC
GAPDH
H3

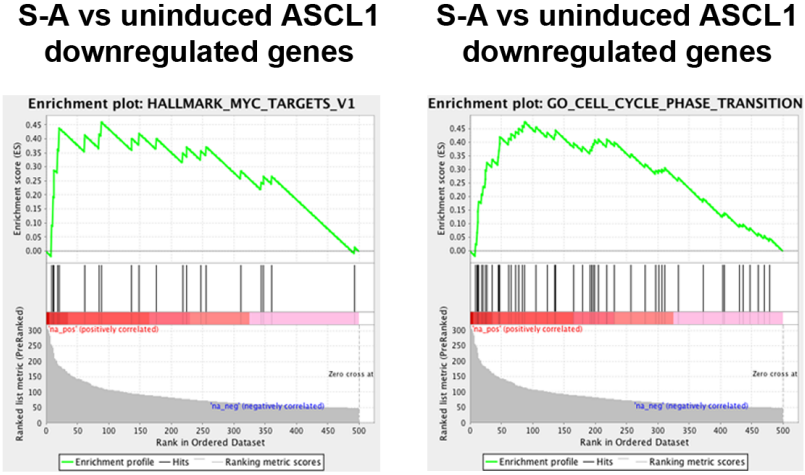
C
S-A vs uninduced ASCL1 downregulated genes
S-A vs uninduced ASCL1 downregulated genes
Enrichment plot: HALLMARK_MYC_TARGETS_V1
Enrichment plot: GO_CELL_CYCLE_PHASE_TRANSITION
Enrichment score (ES)
Ranked list metric (PreRanked)
Rank in Ordered Dataset
Enrichment profile
Hits
Ranking metric scores

Figure 2

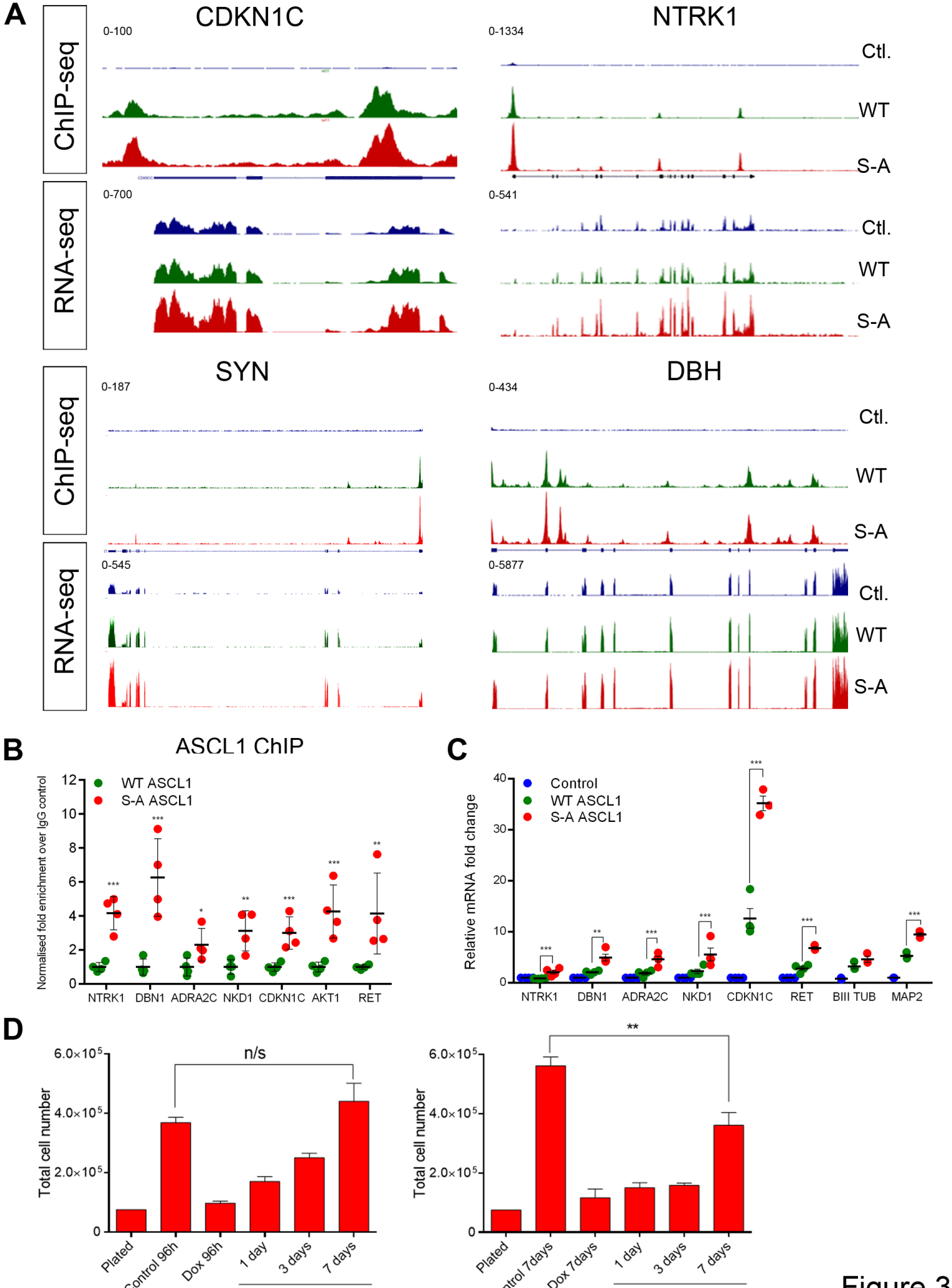
A
ChIP-seq
RNA-seq
CDKN1C
NTRK1
SYN
DBH
0-100
0-700
0-1334
0-541
0-187
0-545
0-434
0-5877
Ctl.
WT
S-A
B
ASCL1 ChIP
WT ASCL1
S-A ASCL1
Normalised fold enrichment over IgG control
NTRK1
DBN1
ADRA2C
NKD1
CDKN1C
AKT1
RET
C
Control
WT ASCL1
S-A ASCL1
Relative mRNA fold change
NTRK1
DBN1
ADRA2C
NKD1
CDKN1C
RET
BIII TUB
MAP2
D
Total cell number
n/s
Plated
Control 96h
Dox 96h
1 day
3 days
7 days
Release
Control 7days
Dox 7days

Figure 3

List of primers used in gene expression qPCR experiments

Gene	Primer forward (5'-3')	Primer reverse (5'-3')
NTRK1	TTGCCTGCCTCTTCCTTTCTAC	ATTGTGGGTTCTCGATGATGTG
DBN1	GAGGAAACTGAGGCAAAGAGGA	TCGGAGCCATCTTCATATGTGT
ADRA2C	GAGTACAACCTGAAGCGCACAC	GGAGGACAGGATGTACCAGGTC
NKD1	AAGAGGAGCGTCCTTGTCAATC	CCGGCGAGATCTAAGTAGTGGT
CDKN1C	GAGCCAATTTAGAGCCCAAAGA	AAGCTTTACACCTTGGGACCAG
RET	TAGCTCCTGGGAGAAGCTCAGT	GGAAAGGAGGTGTTGAAGAAGG
TUBB3	TCAGCAAGGTGCGTGAGGAG	GAGGGTGCGGAAGCAGATGT
MAP2	TTCTGCGCCCAGATTTTATTGA	GCTCCCAATCAATGCTTCCT
DBH	TCAACAACGAGGATGTCTGC	CAGTGTGGAGATGACCTTGG
CDK1	GGCCTTGCCAGAGCTTTTGGAATA	AGTGGTTTCTTAGTTGCTAGTTCAGC
CDK2	TACCGAGCTCCTGAAATCCTCCT	CGGAAGAGCTGGTCAATCTCAGAAT
SKP2	CCACGGAAACGGCTGAAGAGCA	CAAACACCAGAGACCTTTAGCAGCT
E2F1	TGACATCACCAACGTCCTTGAGG	CTGTCGGAGGTCCTGGGTCAA
FOXM1	GTGAATCTTCCTAGACCACCTGGA	GTGACAATTCTCCTTTTCCTCCATCT
BIRC5	CATTCGTCCGGTTGCGCTTTCC	CGGCGCACTTTCTCCGCAGTTT
CDCA7	ACGAACTGGCCGGTATTTTTCATGC	GGTACTCCGCGCTGGAAACTTC
KI67	GAGGTGTGCAGAAAATCCAAA	CTGTCCCTATGACTTCTGGTTGT
PHOX2B	TTCACCAGTGCCCAGCTCAAAGA	TTGCCCGAGGAGCCGTTCTTG
GATA3	CCAGCACAGAAGGCAGGGAGT	CTGTCCGTTCATTTTGTGATAGAGCC
HAND2	ATACGAAGAGGACACTCCCG	GGACCTGATGACTTTCTCCC
TBP	GAGCTGTGATGTGAAGTTTCC	TCTGGGTTTGATCATTCTGTAG

List of primers used in Chip-qPCR experiments

Gene	Primer forward (5'-3')	Primer reverse (5'-3')
SKP2	TGGCCCTTGGAGTGAGTGTATG	ATTGTCCCCTTTCCGCCTGTTA
E2F1	GCCTTCACTTCCCCTAGCAGCT	GTGGTGGGGCTGGGATTTGAAC
CDCA7	GGTCTTGCGAACCGGTCTCCTA	AAATGCACTTAACCACCGCCCG
NTRK1	GATGACCTGGACAGCAACCTTT	GCATTTTTACATTTGGGGAGGA
DBN1	GAGAAGCAGAGGGAGAAACCAG	TGTCCCTTCACTTCTGTCCTTTC
ADRA2C	CACATGTGCTAATGCTCACACC	TGTATCTCCCCACCTGTGTCTG
NKD1	CTTAACAGAGAGGAGGCCCTGA	CAGAGACGTCCAAATGACTTGC
CDKN1C	AGCTTTACACCTTGGGACCAGT	GACCGTTCATGTAGCAGCAACC
RET	CTGATTCCAAAATGAGCACAGG	CCCCAAGTGCTAGGATTACAGG
DBH	CCGCCTGTCTACTTCAACTCC	TGTACATGAAGGCTGCCTCC
PHOX2B	CTTGCTAATGTCTCTGCCTGCG	AGACGCATAGAAACACCCACCA
GATA3	GCAGGGTAAGATGTCCAAAGCC	GGTGAGTGGAAAGGAATTGGAGTC
HAND2	ACTGGAGTTGGAATGAGGCATCT	CTAAGGCTTTCGTGGGGCAATG